Eur. Phys. J. A **5**, 183–190 (1999)

THE EUROPEAN PHYSICAL JOURNAL A

Effects of the nuclear correlations on the neutrino-oxygen interactions

J. Marteau

Institut de Physique nucléaire de Lyon, IN2P3-CNRS et Université Claude Bernard, 43 Bd du 11 Novembre 1918, F-69622 Villeurbanne Cedex, France

Received: 15 January 1999
Communicated by P. Schuck

Abstract. We perform a calculation of the absolute charged current neutrino-oxygen events rates relevant in the atmospheric neutrino experiments. The inclusive reaction cross-section is split into exclusive channels, which are classified according to the number of Čerenkov rings they produce. The model includes the effects of residual interaction in a RPA scheme with both nucleon-hole and Delta-hole excited states and the effects of (*np-nh*) excitations (*n=2,3*). Our result is that although the flavor ratio μ/e remains almost unaffected by the nuclear effects considered here and often neglected in the Monte-Carlo simulations, the absolute events rates are subject to important modifications.

PACS. 13.15.+g Neutrino interactions – 14.40.-n Mesons – 24.30.Gd Other resonances

1 Introduction

Neutrino physics is among the hottest topics of particle physics with the recent indications in favor of neutrino oscillations. After the solar neutrino deficit, the apparent anomaly in the ratio of muon to electron atmospheric neutrinos $R_{\mu/e} = (N_{\nu_\mu} + N_{\bar{\nu}_\mu})/(N_{\nu_e} + N_{\bar{\nu}_e})$ observed by (Super-)Kamiokande [1,2], IMB [3], Soudan-2 [4] and the asymmetry in the zenithal distributions of the $\mu-$ type events in Super-Kamiokande [2] have given a strong support to the oscillation hypothesis: $\nu_\mu \longrightarrow \nu_x$ where $\nu_x = \nu_\tau$ (*i.e. active-active* transition) or $\nu_x = \nu_s$ (*i.e. active-sterile* transition). The solution of the atmospheric neutrinos anomaly in terms of $\nu_\mu \longrightarrow \nu_e$ oscillations has been excluded by the Chooz collaboration [5].

A number of atmospheric neutrinos experiments use large underground water Čerenkov detectors. In these experiments only "one Čerenkov ring" (1 Č.R.) events are retained for the analysis. These events are usually assumed to be produced by quasi-elastic charged current interactions in which a charged lepton is emitted above Čerenkov threshold and leads to one Čerenkov ring. The nucleon which is ejected from the nucleus is in general below threshold and therefore does not produce another ring. The region of energy transfer in processes involving atmospheric neutrinos of ~ 1 GeV extends from the quasi-elastic peak to the Delta resonance region. The evaluation of the nuclear responses in the latter region usually relies on the assumption that the Delta decays into a pion and a nucleon (this is the case for example in [6] where the authors use a relativistic model *à la* Walecka to compute the nuclear response functions). The pion leading to an additional Čerenkov ring, this charged current event belongs to the two Čerenkov rings (2 Č.R.) class and is rejected by the experimental cuts. Thus theoretical calculations are often limited to the quasi-elastic peak which is treated in Fermi gas models or with more elaborate treatments taking into account the shell structure of the oxygen nucleus and RPA type correlations [7].

However the nuclear dynamics is far more complex than this simple picture. Indeed the pion in the nucleus is a quasi-particle with a broad width and can decay for instance into a *particle-hole* excitation. Therefore the decay of a Delta in the nuclear medium can lead to a nucleon and a *particle-hole* state. In such a process, two nucleons are ejected from the nucleus, none of them producing a Čerenkov ring, and the event belongs to the 1 Č.R. class. Furthermore (*2p-2h*) states may also be directly excited in the nucleus without excitation of the Delta resonance. This process also results in the emission of two nucleons and the event belongs to the 1 Č.R. class. Following these arguments, we perform a full calculation of the neutrino-oxygen cross sections beyond the quasi-elastic assumption, with the identification of the possible final states. This procedure leads to a complete evaluation of the 1 Č.R. events yields in the atmospheric neutrinos experiments and its impact in the description of the retained neutrino events in the detectors has to be investigated.

The starting point of this calculation is the inclusive charged current cross section for the reaction
$\nu_l\,(\bar{\nu}_l) + {}^{16}\mathrm{O} \longrightarrow l^-\,(l^+) + X$,

$$\frac{\partial^2\sigma}{\partial\Omega\partial k'} = \frac{G_F^2\,\cos^2\theta_c\,(\boldsymbol{k}')^2}{2\,\pi^2}\,\cos^2\frac{\theta}{2}\,\Bigg[G_E^2\,(\frac{q_\mu^2}{\boldsymbol{q}^2})^2\,R_\tau^{NN} + G_A^2\,\frac{(M_\Delta - M)^2}{2\,\boldsymbol{q}^2}\,R_{\sigma\tau(L)}^{N\Delta} + G_A^2\,\frac{(M_\Delta - M)^2}{\boldsymbol{q}^2}R_{\sigma\tau(L)}^{\Delta\Delta} + (G_M^2\,\frac{\omega^2}{\boldsymbol{q}^2} + G_A^2)\,(-\frac{q_\mu^2}{\boldsymbol{q}^2} + 2\tan^2\frac{\theta}{2})\,\times (R_{\sigma\tau(T)}^{NN} + 2R_{\sigma\tau(T)}^{N\Delta} + R_{\sigma\tau(T)}^{\Delta\Delta}) \pm 2\,G_A\,G_M\,\frac{k+k'}{M}\,\tan^2\frac{\theta}{2}\,\times (R_{\sigma\tau(T)}^{NN} + 2R_{\sigma\tau(T)}^{N\Delta} + R_{\sigma\tau(T)}^{\Delta\Delta})\Bigg] \quad (1)$$

where G_F is the weak coupling constant, θ_c the Cabbibo angle, k and k' the initial and final lepton momenta, $q_\mu = k_\mu - k'_\mu = (\omega, \boldsymbol{q})$ the four momentum transferred to the nucleus, θ the scattering angle, M_Δ (M) the Delta (nucleon) mass. The plus (minus) sign in (1) stands for the neutrino (antineutrino) case. In a provisional approximation, to be lifted after, we have neglected in (1) the lepton masses and we have kept the leading terms in the development of the hadronic current in p/M, where p denotes the initial nucleon momentum. The electric, magnetic and axial form factors are taken in the standard dipole parameterization with the following normalizations: $G_E(0) = 1.0$, $G_M(0) = 4.71$ and $G_A(0) = 1.25$. We have introduced the inclusive *isospin* (R_τ), *spin-isospin longitudinal* ($R_{\sigma\tau(L)}$) and *spin-isospin transverse* ($R_{\sigma\tau(T)}$) nuclear responses functions (the longitudinal and transverse character of these last two responses refers to the direction of the spin operator with respect to the direction of the transferred momentum):

$$R_\alpha^{PP'} = \sum_n \langle n|\sum_{j=1}^{A} O_\alpha^P(j)\,e^{i\,\boldsymbol{q}.\boldsymbol{x}_j}|0\rangle\,\times \langle n|\sum_{k=1}^{A} O_\alpha^{P'}(k)\,e^{i\,\boldsymbol{q}.\boldsymbol{x}_k}|0\rangle^*\,\delta(\omega - E_n + E_0) \quad (2)$$

where the operators have the following forms:

$$O_\alpha^N(j) = \tau_j^\pm,\ \ (\boldsymbol{\sigma}_j.\widehat{q})\,\tau_j^\pm,\ \ ((\boldsymbol{\sigma}_j \times \widehat{q}) \times \widehat{q})\,\tau_j^\pm,$$

for $\alpha = \tau$, $\sigma\tau(L)$, $\sigma\tau(T)$, and

$$O_\alpha^\Delta(j) = (\boldsymbol{S}_j.\widehat{q})\,T_j^\pm,\ \ ((\boldsymbol{S}_j \times \widehat{q}) \times \widehat{q})\,T_j^\pm,$$

for $\alpha = \sigma\tau(L)$, $\sigma\tau(T)$. In the above expressions, the superscript P ($P = N$ or Δ) denotes the type of the *Particle-hole* excitations (*Nucleon-hole* or *Delta-hole*) induced by the operator O_α^P. The operators S and T are the usual $1/2$ to $3/2$ transition operators in the spin and isospin space (for instance see [10]). In this work we neglect the small quadrupole transition connecting the nucleon to the Delta through the pure isospin operator, therefore the isospin response just involves nucleon-hole excitations. Note that we have assumed the existence of a scaling law between the nucleon and Delta magnetic and axial form factors [11]:

$$G_M^*/G_M = G_A^*/G_A = f^*/f,$$

where f^* (f) is the $\pi\,N\,\Delta$ ($\pi\,N\,N$) coupling constant. For a matter of convenience, we have incorporated the scaling factor $f^*/f = 2.2$ into the responses.

2 Formalism

The evaluation of the nuclear responses is performed within the model developed by Delorme and Guichon for the interpretation of the (^{3}He, t) charge exchange experiments [12,13]. In this model the polarization propagators $\Pi^0(\omega, \boldsymbol{q}, \boldsymbol{q}')$ without nuclear correlations are evaluated in a semi-classical approximation to properly take into account the finite size effects. This implies the use of a local Fermi momentum $k_F(r)$ which is calculated by the means of an experimental nuclear density: $k_F(r) = \sqrt[3]{3/2\,\pi^2\,\rho(r)}$. Note that this procedure differs a little from the pure semi-classical one [1] but it has been found to give better results for the $\pi -$ nucleus reactions. The "bare" polarization propagators Π^0 (in the following "bare" will mean that the nuclear correlations are switched off) are then used as an input to exactly solve the RPA equations in the ring approximation, as we will develop in the following. In [12,13] the authors gave satisfactory fits to the set of the experimental data. This model was also confronted to the pion-nuclei experimental results [14] and the agreement obtained for the total and elastic cross sections was remarkably good.

As mentioned above, the first step of the calculation is the evaluation of the bare polarization propagators. A crucial ingredient of the model is the Delta resonance width modified by the nuclear effects. We adopt the parameterization of [15] where the Delta width is split into the contributions of different decay channels: the "quasi-elastic" channel, $\Delta \longrightarrow \pi\,N$, modified by the Pauli blocking of the nucleon and the distortion of the pion, the two-body (*2p-2h*) and three-body (*3p-3h*) absorption channels. This parameterization leads to a good description of pion-nuclear reactions. At resonance we find a Delta width around 130 MeV, a value rather close to the free case. This value reflects the importance of the two- and three-body absorption channels which are large enough to counteract the effect of the Pauli blocking and lead to this overall enhancement of the Delta width. Note furthermore that at resonance the "quasi-elastic" channel modified by the medium effects, is almost equal to the free "quasi-elastic" one. The model of Delorme and Guichon also accounts for the (*2p-2h*) excitations which are not reducible to a modified Delta width. The evaluation of such processes is performed by extrapolating the calculations of two-body pion absorption at threshold given in [16]. We have limited ourselves to the imaginary part of these two-body polarization

[1] For a pure quantum approach in the low energy part of the nuclear response, applied in the context of terrestrial neutrinos experiments, see [8,9]

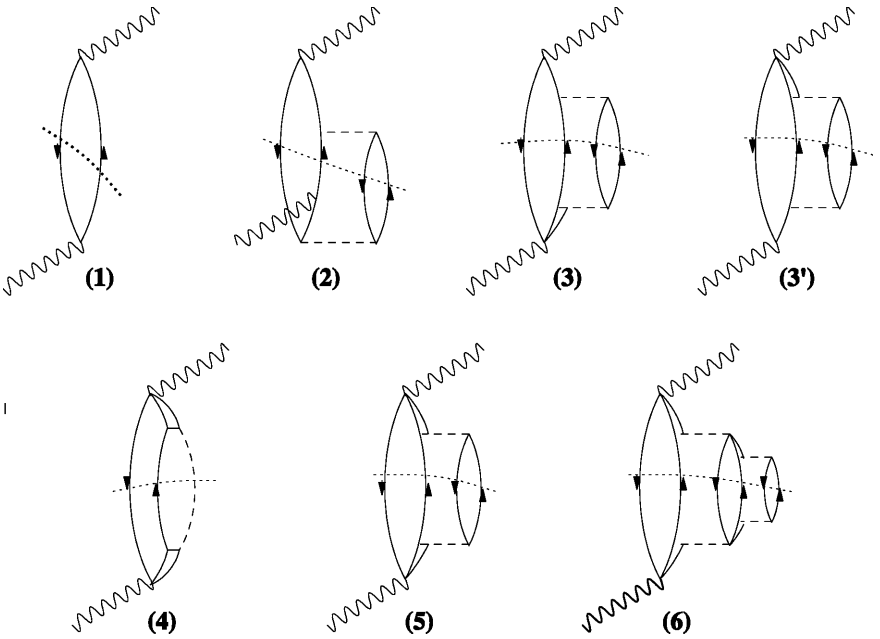

Fig. 1. Feynman graphs of the partial polarization propagators: NN quasi-elastic (1), NN (2p-2h) (2), $N\Delta$ (2p-2h) (3), ΔN (2p-2h) (3'), $\Delta\Delta$ (πN) (4), $\Delta\Delta$ (2p-2h) (5), $\Delta\Delta$ (3p-3h) (6). The conventions for the various lines drawings are given in the text

propagators, the comparison with experimental data such as pion-nucleus scattering or (e, e') scattering giving satisfactory results to that order of approximation. By construction, the bare polarization propagator $\Pi^0(\omega, \boldsymbol{q}, \boldsymbol{q}')$ is the sum of the following partial components:

1. NN quasi-elastic (the standard Lindhard function),
2. NN (*2p-2h*),
3. $N\Delta$ and $3'$. ΔN (*2p-2h*),
4. $\Delta\Delta$ ($\pi\, N$),
5. $\Delta\Delta$ (*2p-2h*),
6. $\Delta\Delta$ (*3p-3h*),

where the notation N (Δ) stands for Nucleon-hole (Delta-hole) states as previously. The Feynman graphs corresponding to these partial polarization propagators are displayed on Fig. 1 with the following conventions: the wiggled lines represent the external probe, the full lines correspond to the propagation of a nucleon (or a hole), the double lines to the propagation of a Delta, the dashed lines to an effective interaction between nucleons and/or Deltas. Finally the dotted lines indicate which intermediate state has to be placed on-shell to obtain the desired partial nuclear response. Note that in the case of (np-nh) polarization propagators the number of graphs is large and we just give one example in the figure.

The bare responses are then given by the standard relations:

$$R^0_{(k)}(\omega, q) = -\frac{1}{\pi}\,\mathrm{Im}(\Pi^0_{(k)}(\omega, q, q)), \tag{3}$$

with the obvious sum rule:

$$R^0(\omega, q) = -\frac{1}{\pi}\,\mathrm{Im}(\Pi^0(\omega, q, q)) = \sum_{k=1}^{n_k} R^0_{(k)}(\omega, q), \tag{4}$$

where n_k denotes the number of partial reaction channels ($n_k = 7$ in our model).

Following the method detailed in [12,13] we include the effects of nuclear correlations by exactly solving the RPA equations in the ring approximation. For instance the inclusive RPA polarization propagators $\Pi(\omega, \boldsymbol{q}, \boldsymbol{q}')$ are solution of the generic equation:

$$\Pi = \Pi^0 + \Pi^0\, V\, \Pi \tag{5}$$

where V denotes the effective interaction between *particle-hole* excitations and $\Pi^0(\omega, \boldsymbol{q}, \boldsymbol{q}')$ the inclusive bare polarization propagator calculated previously and used here as an input. In the spin-isospin channel the RPA equations couple the L, T and the N, Δ components of the polarization propagators. For the effective interaction relevant in the isospin and spin-isospin channels, we use the standard $\pi + \rho + \delta -$ function parameterization:

$$\begin{aligned} V_{NN} &= (f' + V_\pi + V_\rho + V_{g'})\ \boldsymbol{\tau}_1.\boldsymbol{\tau}_2 \\ V_{N\Delta} &= (V_\pi + V_\rho + V_{g'})\ \boldsymbol{\tau}_1.\boldsymbol{T}_2^\dagger \\ V_{\Delta N} &= (V_\pi + V_\rho + V_{g'})\ \boldsymbol{T}_1.\boldsymbol{\tau}_2 \\ V_{\Delta\Delta} &= (V_\pi + V_\rho + V_{g'})\ \boldsymbol{T}_1.\boldsymbol{T}_2^\dagger \end{aligned} \tag{6}$$

where in the NN case, for example (the $N\Delta$, ΔN and $\Delta\Delta$ cases are obtained with the appropriate replacements $\sigma \longrightarrow S$):

$$\begin{aligned} V_\pi &= F_\pi^2\ \left(\frac{\boldsymbol{q}^2}{\omega^2 - \boldsymbol{q}^2 - m_\pi^2}\right)\ (\boldsymbol{\sigma}_1.\widehat{q})\ (\boldsymbol{\sigma}_2.\widehat{q}) \\ V_\rho &= F_\rho^2\ \left(\frac{\boldsymbol{q}^2}{\omega^2 - \boldsymbol{q}^2 - m_\rho^2}\right)\ (\boldsymbol{\sigma}_1 \times \widehat{q})\,.\,(\boldsymbol{\sigma}_2 \times \widehat{q}) \\ V_{g'} &= F_\pi^2\ g'\ \boldsymbol{\sigma}_1.\boldsymbol{\sigma}_2 \end{aligned} \tag{7}$$

In the preceding equations, $F_\pi(q)$ and $F_\rho(q)$ are the standard pion-nucleon and rho-nucleon form factors. The values we adopt for the relevant parameters can be found in

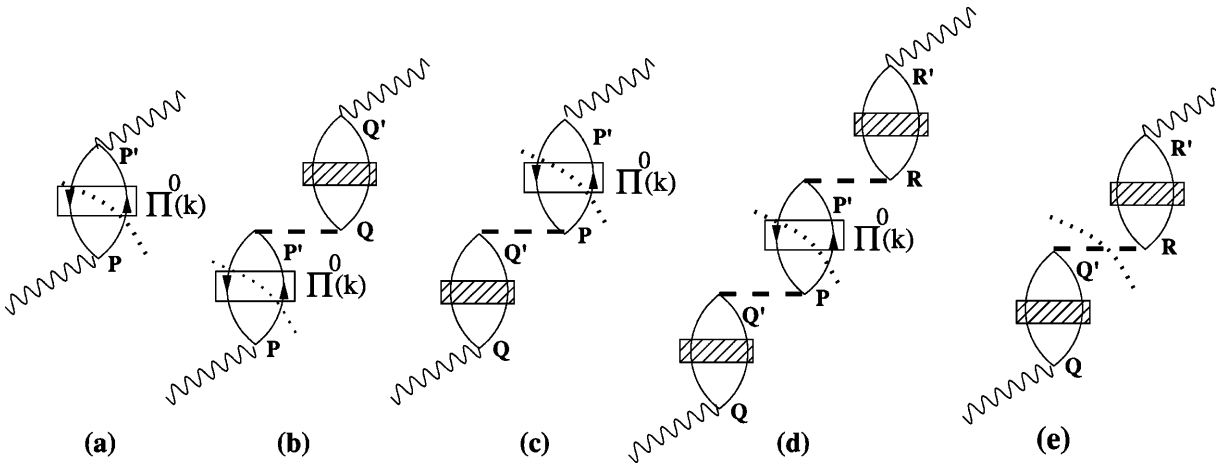

Fig. 2. Graphic representation of the partial RPA response functions. (a)-(d): incoherent partial response functions. (e): coherent partial response function. The hatched rings correspond to the inclusive RPA polarization propagator, the free rings to the partial bare polarization propagators, the dashed line to the effective interaction and the dotted line indicates which intermediate state is placed on-shell

[14]. In particular we take the "common" Landau-Migdal parameters:

$$f' = 0.6,\ g'_{NN} = 0.7,\ g'_{N\Delta} = g'_{\Delta N} = 0.5,\ g'_{\Delta\Delta} = 0.5$$

The inclusive RPA responses functions are deduced from the corresponding inclusive RPA polarization propagators by the usual relation:

$$R(\omega, q) = -\frac{1}{\pi}\,\mathrm{Im}(\Pi(\omega, q, q)) \tag{8}$$

We perform the calculation of the partial RPA responses as follows. Starting from the RPA equation (5), we write the imaginary part of $\Pi(\omega, \boldsymbol{q}, \boldsymbol{q'})$ in the following form:

$$\mathrm{Im}(\Pi) = |1 + \Pi\, V|^2\,\mathrm{Im}(\Pi^0) + |\Pi|^2\,\mathrm{Im}V \tag{9}$$

with $\mathrm{Im}(\Pi^0) = \sum_{k=1}^{n_k} \mathrm{Im}(\Pi^0_{(k)})$. This sum rule gives the different contributions to the inclusive RPA response functions. The first terms in (9) are reminiscent of the bare case. Indeed we recognize the bare partial response functions (apart from the trivial $-\pi$ factor) corrected by a factor involving the inclusive RPA polarization propagator and the effective interaction. The partial RPA response functions, defined by:

$$R_{(k)}(\omega, q) = -\frac{1}{\pi}\,|1 + \Pi\, V|^2\,\mathrm{Im}(\Pi^0_{(k)}(\omega, q, q)) \tag{10}$$

are represented by the graphs (a) to (d) on Fig. 2, where the hatched rings correspond to the inclusive polarization propagator solution of (5), the non hatched rings to the bare partial polarization propagators (the dotted line means that we take the imaginary part of these propagators) and the dashed lines to the effective interaction. It is easy to recover on these graphs the different terms of the development of (10). Note that in the RPA case, a PP' reaction channel ($P, P' = N, \Delta$) gets contributions from every QQ' configurations (NN, $N\Delta$, ΔN, $\Delta\Delta$). The last term in (9) corresponds to the "coherent" response function:

$$R_{coh}(\omega, q) = -\frac{1}{\pi}\,|\Pi|^2\,\mathrm{Im}V \tag{11}$$

It is absent of the response spectrum when the effective interaction is switched off. In the domain of energy considered here the sole contribution to this channel comes from the pion exchange. This process corresponds to the emission of a pion on its mass-shell, the nucleus remaining in its ground state. It is represented by the graph (e) on Fig. 2 where the dashed line stands for the exchange of a pion. The implications of these partial reaction channels will be discussed in the following sections.

3 Cross sections

The next step is the calculation of the neutrino-oxygen cross section. The doubly differential cross section is given in a first approximation by (1). Our final calculation relies on a more complete expression, which we will briefly describe in the following, but the main features remain unchanged. First it is essential to note that the neutrino-nucleus reaction is strongly dominated by the transverse spin-isospin channel. This is clear from (1). Indeed the terms multiplying the transverse responses, depending on the axial and magnetic form factors, have a much larger magnitude than for the longitudinal case. Furthermore the NN quasi-elastic spin-isospin longitudinal response is totally suppressed in the cross section. This suppression arises from an exact cancellation at the top of the quasi-elastic peak between the various terms entering the contraction of the leptonic and the hadronic tensors. This suppression is only partial in the Delta resonance or in the "dip" region (the region intermediate between the quasi-elastic and the Delta peaks). This result is in contradiction with the study of [17] where the relative weights

of the transverse to the longitudinal responses were assumed to be 2:1. Note however that the suppression of the NN longitudinal response is no more exact when one considers the complete expression of the doubly differential cross section, which includes the terms involving the charged lepton mass (in fact we consider only the muon mass) and the terms up to order $(p/M)^2$ in the reduction of the hadronic current. The contributions of the NN longitudinal response are then of order $(m_l/M)^2$, where m_l denotes the mass of the charged lepton, and of order (p/M). These corrections are rather weak. As another source of corrections we have also considered the renormalization of the axial charge by the mesonic exchange currents, because the suppression of the NN longitudinal response involves the time component of the axial current. Following the parameterization of [18] we make the replacement $g_A \longrightarrow g_A(1+\delta)$ in the time component of the axial current. The contribution of the NN longitudinal response is then of order δ^2. Even with the relatively high value $\delta \sim 0.5$ suggested in [19], the contribution of the NN longitudinal response remains weak. The same conclusion holds for the $N\Delta$ and $\Delta\Delta$ longitudinal responses which are widely dominated by the corresponding transverse ones. Note that in the antineutrino-nucleus reactions the weight of the transverse channel is somewhat reduced because of the change in sign in the interference term. However even in this case, the transverse responses correspond to 75 % of the total, the remaining arising essentially from the NN pure isospin response.

We will now investigate the implications of these global features on the simply differential cross section $\partial\sigma/\partial k'$, which is obtained from the doubly differential cross section by a numerical integration over the solid angle. The great interest of our method is the separation of the inclusive cross section into partial contributions. This separation is simply achieved by the replacement, in the expression of the cross section, of the inclusive response functions with the "exclusive" ones, calculated in the previous section. The results are shown on Fig. 3 which displays the simply differential cross section versus the energy transfer, fixing for the sake of illustration a neutrino energy of 700 MeV.

The inclusive cross section is given by the thick curve. It gets its main contribution from the NN quasi-elastic channel (thin full line) which peaks at relatively low energy transfer. For the sake of comparison we have shown the contribution of the NN quasi-elastic channel without RPA (thin long dashed line). We observe that the cross section is reduced and hardened in the RPA case. This result is in full agreement with that of [7]. The shift in strength reflects the dominance of the transverse response. Indeed the Landau-Migdal interaction is repulsive for all values of the transfer and the $\rho-$exchange piece is not attractive enough in the domain of energy considered here to counteract this feature. This repulsive effective interaction hardens and reduces the transverse response functions. For instance this conclusion no longer holds in the longitudinal channel where the $\pi-$exchange is attractive enough to overcome the Landau-Migdal interaction and to create a collective mode (the so-called *pionic branch* [12, 13]). But, as we mentioned previously, the suppression of the longitudinal channel makes the neutrino a poor probe of this pionic mode.

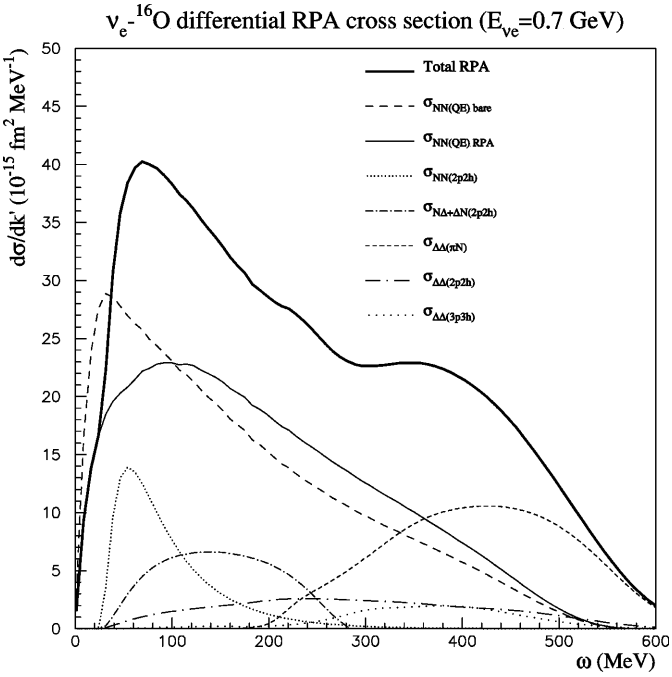

Fig. 3. Differential charged current $\nu_e - {}^{16}$O interactions cross-section versus the energy transfer. The thick curve represents the inclusive cross-section. The following exclusive contributions to the inclusive cross-section are displayed: NN (quasi-elastic) (full thin curve), NN (2p-2h) (short dotted curve), $N\Delta + \Delta N$ (2p-2h) (short dot-dashed curve), $\Delta\Delta$ (πN) (short dashed curve), $\Delta\Delta$ (2p-2h) (long dot-dashed curve) and $\Delta\Delta$ (3p-3h) (long dotted curve). Also shown is the "bare" NN quasi-elastic cross-section (long dashed curve)

The effect of the RPA correlations are less strong in the others channels and are not shown here. The $\Delta\Delta$ (πN) channel (short dashed curve on the figure) arises at high energy transfer ($\omega \sim 450$ MeV). This is in good agreement with the result of the relativistic calculations given in [6] where the Delta was taken into account as a free resonance and where the RPA correlations did not include Delta-hole configurations. The agreement between the two calculations is not surprising. Indeed we use relativistic kinematics for the evaluation of the polarization propagators as in [12–14] and we include the terms up to second order in the (p/M) reduction of the hadronic current as mentioned above. Furthermore the RPA effects on the transverse response in the Delta region, that is at high transfer, are somewhat reduced in the cross section by the form factors and the differences between RPA and bare transverse response functions are very weak at these values of the transfer. Thus our calculations show that a free Delta resonance gives a rather good approximation of the $\Delta\Delta$ (πN) (or "quasi-elastic") channel. This result corroborates the fact that the "quasi-elastic" Delta width in the nuclear medium is close to its free value, the Pauli

blocking being cancelled by the other mechanisms taken into account.

The most interesting feature of the cross section is the importance of the (*np-nh*) channels. The kinematics of the neutrino-nucleus reaction tends to favor the NN (*2p-2h*) channel (short dotted curve) which peaks at low energy transfer. However the $N\Delta + \Delta N$ (*2p-2h*) channel (short dot-dashed curve) gives a rather large contribution to the inclusive cross section and has an extended spectrum in the "dip" region. Its importance has been pointed out in the (e, e') scattering where it is necessary to reproduce the experimental data in the "dip" region (for example see [20]). Finally note that the $\Delta\Delta$ (*2p-2h*) (long dot-dashed curve) and (*3p-3h*) (long dotted curve) spectra extend over a wide range of energy transfer, while the $\Delta\Delta$ (πN) channel is concentrated in the so-called Delta peak. They give a little contribution to the inclusive cross section (in particular the (*3p-3h*) channel is rather weak) but the extension of their spectra will have important consequences in the specific events yields.

The results obtained in this section show that the inclusive neutrino-oxygen cross section is strongly modified with respect to the free NN quasi-elastic case, which is quite often the sole channel entering into the calculations. In particular we have seen the occurrence of large contributions from the two- and three-body channels. The main effect of the nuclear correlations is the hardening of the NN quasi-elastic channel. They have rather low impact on the others reaction channels and therefore could be legitimately neglected.

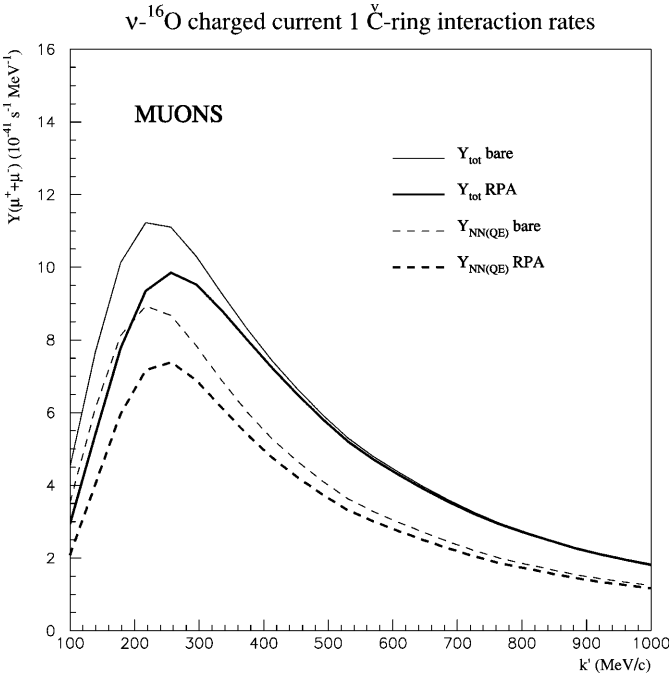

Fig. 4. One Čerenkov $(\nu_\mu + \bar{\nu}_\mu) - {}^{16}$O events yields versus the muon momentum. The full curves correspond to the total 1 Č.R. events yields with (thick curve) and without (thin curve) RPA. The dashed curves correspond to the NN quasi-elastic 1 Č.R. events yields with (thick curve) and without (thin curve) RPA

4 Events yields

In this section we compute numerically the neutrino-oxygen events yields for a fixed charged lepton momentum:

$$Y_{(\nu_\alpha+\bar{\nu}_\alpha)}(k') = \int_{E_{k'}}^{\infty} dE \left(\Phi_{\nu_\alpha}(E) \frac{\partial\sigma}{\partial k'}(E,k') + \Phi_{\bar{\nu}_\alpha}(E) \frac{\partial\bar{\sigma}}{\partial k'}(E,k') \right) \quad (12)$$

where E is the neutrino energy, Φ_ν ($\Phi_{\bar{\nu}}$) the incoming neutrinos (antineutrinos) flux and $\partial\sigma/\partial k'$ ($\partial\bar{\sigma}/\partial k'$) the neutrino-oxygen (antineutrino-oxygen) cross section computed in the previous section. We use the fluxes of Bartol [21] in our calculations for the sake of comparison with the results of [7]. The main feature of these fluxes is their sharp decrease with increasing neutrino energy. Note that several theoretical attempts have been undertaken to compute these atmospheric neutrinos fluxes. The sources of possible differences between three models have been analyzed in [22]. The predictions of these models on the flavor ratio agree at a ~ 5 % degree of accuracy. Anyway the discrepancies in the absolute fluxes remain rather large ($\sim$ 20 %). Furthermore new measurements on the primary cosmic rays fluxes could lead to some modifications with respect to the present situation. The cumulated uncertainties on the neutrino fluxes and on the neutrino-oxygen cross sections could lead to modifications in the experimental analysis, even if they remain unlikely to explain the atmospheric neutrinos anomaly. To perform an analysis of the events yields, we need to classify the partial reaction channels according to the number of Čerenkov ring(s) they produce. This classification has been elaborated within a few rough assumptions. First we consider that every nucleon ejected from the nucleus remains under Čerenkov threshold. In water, the threshold kinetic energy for a particle of mass m is $E \sim 0.5\,m$. For a nucleon, produced through Delta decay or (*2p-2h*) mechanisms, the assumption is fairly good. On the opposite, we assume that every pion which escapes the nuclear medium produces a Čerenkov ring. The threshold energy for a pion being $\sim$ 70 MeV, this assumption is believed to be reliable. Then the partial reaction channels leading to one Čerenkov ring, in charged current interactions, are the NN quasi-elastic one, which is usually taken into account in the simulations, and the (*np-nh*, n>1) type channels (both NN, $N\Delta$, ΔN and $\Delta\Delta$). The remaining reaction channels, $\Delta\Delta$ (πN) and coherent pion production, are supposed to lead to at least two Čerenkov rings. The results for the 1 Č.R. events yields, which are relevant in the atmospheric neutrino experiments, are shown on Fig. 4 for incident ν_μ and $\bar{\nu}_\mu$, the full curves corresponding to the total 1 Č.R. events yields and the dashed curves to the sole NN quasi-elastic 1 Č.R. events yields. We give the results of the calculations without (thin curves) and with (thick curves) RPA.

First we observe that the RPA tends to reduce the events yields. This is not hard to understand. Indeed the RPA tends to harden the cross sections, *i.e.* to push the strength towards higher energies. But the fluxes decrease with increasing energies and therefore the higher energies are disfavored. This reduction affects mostly the NN quasi-elastic channel in accordance with the result obtained for reaction cross sections. The maximal reduction factor is of the order of 10 %. A more interesting feature is the strong enhancement of the absolute events yields implied by the (*np-nh*) channels. At the maximum value of the yields, the enhancement of the total yield with respect to the NN quasi-elastic one is around 30 %. This result reflects the main features of the cross sections. Furthermore one must be aware that this result is a lower limit of the true enhancement. Indeed we know that pions can be re-absorbed in the nucleus. Therefore the events produced in the $\Delta\Delta$ (πN) channel can also lead to one Čerenkov ring if the pion does not escape from the nucleus. Thus we can conclude that the RPA 1 Č.R. events yields induced by charged current interactions is globally enhanced with respect to the NN quasi-elastic 1 Č.R. events yields without RPA. The difference between the two calculations could be responsible for the small discrepancy between the experimental and simulated events distributions in Super-Kamiokande [2]. But we need complementary informations to ensure this conclusion. Indeed it is hard to establish the enhancement factor firmly. Our present analysis leads to a maximum enhancement factor of the order of $\sim$ 20 %. We have already mentioned that the problem of pion absorption, which is not yet considered in our calculations, could still enhance this factor. We should also be aware that there exists some misidentification problems which could have a more or less large effect. One of the misidentification source, pointed out by the authors of [6], is the "coherent" pion production. Their analysis is based on the assumption that the forward peaked angular distribution of the coherent pions entails the coherent pions to be emitted with a small angle with respect to the charged lepton direction. This could mimic a "shower" which could be interpreted as an $e-$type event, whatever may be the flavor of the incoming neutrino. Our calculations show that this coherent channel brings a tiny contribution (less than 2 % of the total $\nu_e + \bar{\nu}_e$ events yield) which makes it irrelevant in the atmospheric neutrino anomaly. The suppression of this channel is understandable. Part of it is due to the nuclear form factors effects as discussed for example in [10]. In addition the coherent response manifests itself mainly in the longitudinal spin-isospin channel and we have seen that this channel is suppressed with respect to the transverse one in the neutrino-nucleus reactions. The coherent pions should not be a problem.

The case of the neutral currents is less clear. In charged current interactions, pions ("coherent" or not) lead to, at least, 2 Č.R. events and are excluded from the analysis. But in neutral currents interactions they lead to 1 Č.R. events, because the scattered neutrino does not produce any ring. We have computed the neutral current events yields in each reaction channel, the few differences with respect to the charged current case being easily included in the formalism. The problem arising then is the classification of these $\pi-$ like 1 Č.R. events. Indeed in absence of indication on the experimental π/lepton discrimination efficiency in the water Čerenkov experiments, it is not possible to draw firm conclusions on the role played by the neutral currents. This problem has to be investigated further.

Table 1. Comparison of the total and NN quasi-elastic 1 Č.R. events yields ratios for four lepton momentum

k' (MeV/c)	$R_{\mu/e}(NN\,q.e.)/R_{\mu/e}(Total)$
100	1.060
150	1.040
250	0.999
400	1.001

Finally we study the evolution of the flavor ratio with the charged lepton momentum:

$$R_{\mu/e}(k') = Y_{(\nu_\mu+\bar{\nu}_\mu)}/Y_{(\nu_e+\bar{\nu}_e)}, \tag{13}$$

where Y denotes the events yields defined by (12). We compare the total 1 Č.R. events yields flavor ratio with the NN quasi-elastic 1 Č.R. events yields flavor ratio. The result is shown in Table 1 where the ratio of ratios has been calculated for four relevant lepton momentum. There is almost no modification between the two situations. This conclusion strengthens the usual assumption that uncertainties due to nuclear effects cancel when one considers ratios of events rates. Here the maximum effect on the flavor ratio is less than 10 %.

We conclude this work by mentioning the problem of pion emission in neutrino-oxygen interactions. On one side we have shown that the cross sections of the $\Delta\Delta$ (*2p-2h*) and (*3p-3h*) partial channels, which do not not lead to pion emission (*non pionic* channels), extend over a broad region in transfer energy, while the *pionic* channel $\Delta\Delta$ (πN) is peaked at high transfer energy (see Fig. 3). On the other side the neutrino flux lowers the weight of the high energies and favors the low energy components of the spectrum. Then the pionic $\Delta\Delta$ channel will be more suppressed by the incident neutrino flux than the non pionic one. This result is shown on Fig. 5 where the total $\Delta\Delta$ events yield (full thick curve) is split into its three contributions: (πN) (full thin curve), *2p-2h* (dashed curve), *3p-3h* (dotted curve) in the case of $\mu-$ type events.

The main result is that the fraction of the non pionic channels over the pionic one is around 50 %. This result remains valid for every values of the lepton momentum. Thus the (*np-nh*) excitations play an important role in the events yields although their reaction cross sections are relatively low. Finally we would like to point out that some pion production mechanisms, which do not reduce to a simple response function, are still absent of our formalism. For example we have omitted in the production through

[2] We thank Y. Declais for attracting our attention on this point.

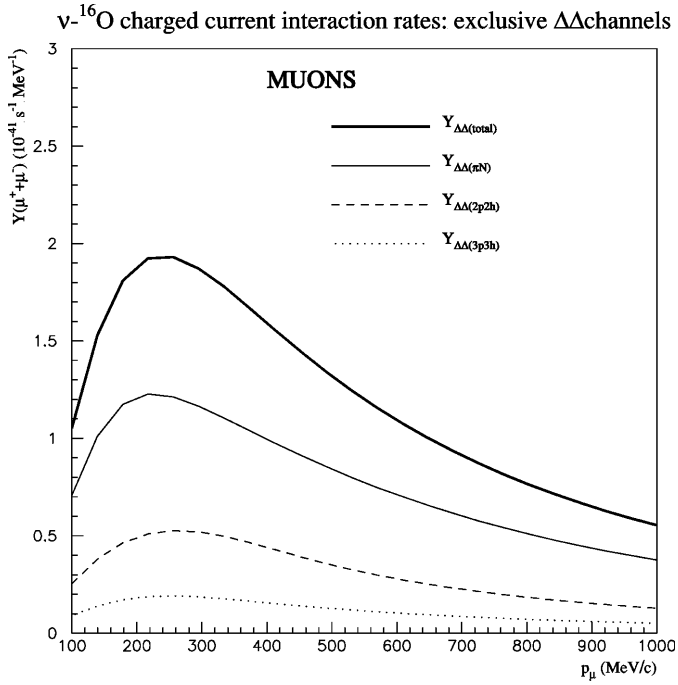

Fig. 5. Contributions to the total $\Delta\Delta$ events yield (full thick curve) of the partial channels: (πN) (full thin curve), (2p-2h) (dashed line), (3p-3h) (dotted line)

the vector current, the Kroll-Ruderman and the pion-in-flight terms which play an important role. Improvements to our present calculations are in progress. Nevertheless these limitations of our present calculations do not alter the need of including the effects of the partial $\Delta\Delta$ (np-nh) reaction channels to avoid an overestimation of the number of pions effectively produced in the neutrino-oxygen interactions.

5 Conclusion

In this work we have studied the effects of nuclear correlations on the charged current neutrino-oxygen cross sections and events yields in specific exclusive reaction channels. We have shown that besides the quasi-elastic channel the (np-nh, n=2,3) excitations also lead to one Čerenkov ring events, which are retained for the analysis of the experiments using large underground water Čerenkov detectors. The enhancement in the one Čerenkov ring events yields is large and could still be increased when some processes, such as pion absorption in nuclei or neutral currents events, are taken into account. It is therefore important to take these nuclear effects into account to perform a calculation of absolute events yields. We have also shown that the flavor ratio $R_{\mu/e}$ is not significantly altered. We have applied our model to other neutrino-nucleus reactions. In particular we have studied the case of iron which is the target-nucleus in the neutrino experiments using calorimeters. The conclusion on the cross sections are the same than the one presented here in the case of oxygen. However such experiments measure more detailed observables than the water Čerenkov detectors, like the energy and momentum spectra of the particles in the final state. The description of these experiments requires the extension of our model. The present work already shows the necessity of taking into account nuclear correlations involving multi-nucleon excitations.

We wish to gratefully acknowledge J. Delorme for his numerous contributions to this work. We are indebted for enlightening discussions and critical reading of the manuscript to J. Delorme, M. Ericson and G. Chanfray. We also thank Y. Declais, P. Lipari and S. Katsanevas for stimulating discussions.

References

1. Y. Fukuda *et al.*, Phys. Lett. B**335**, 237 (1994); K.S. Hirata *et al.*, Phys. Lett. B**280**, 146 (1992)
2. Y. Fukuda *et al*, Phys. Lett. B**433**, (1998) 9; Phys. Rev. Lett. **81**, (1998) 1562
3. R. Becker-Szendy *et al.*, Nucl. Phys. B**38**, 331 (1995); Phys. Rev. D**46**, 3720 (1992)
4. W.W.M. Allison *et al.*, Phys. Lett. B**391**, 491 (1997)
5. M. Apollonio *et al.*, Phys. Lett. B**420**, 397 (1998)
6. H. Kim, S. Schramm, C.J. Horowitz, Phys. Rev. C**53**, 3131 (1996)
7. J. Engel, E. Kolbe, K. Langanke, P. Vogel, Phys. Rev. D**48**, (1993) 3048
8. N. Auerbach, N. Van Giai, O.K. Vorov, Phys. Rev. C**56**, 2368 (1997)
9. E. Kolbe, K. Langanke, S. Krewald, F.K. Thielemann, Nucl. Phys. A**450**, 599 (1992); E. Kolbe, K. Langanke, F.K. Thielemann, P. Vogel, Phys. Rev. C**52**, 3437 (1995)
10. T. Ericson, W. Weise, *Pions and nuclei*, Oxford Science Publications, 1988
11. G.F. Low, *et al*, Phys. Rev. **106**, (1957) 1345
12. J. Delorme, P.A.M. Guichon, in *Proceedings of* 10^e *biennale de physique nucléaire, Aussois, march 6-10, 1989*, rapport LYCEN 8906, p. C.4.1, also in the *Proceedings of the 5th french-japanese symposium on nuclear physics, Dogashima, Izu, september 26-30, 1989*, edited by K. Shimizu and O. Hashimoto, p. 66
13. J. Delorme, P.A.M. Guichon, Phys. Lett. B **263**, 157 (1991)
14. I. Laktineh, W.M. Alberico, J. Delorme, M. Ericson, Nucl. Phys. A**555**, (1993) 237
15. E. Oset, L.L. Salcedo, D. Strottman, Phys. Lett. **165**B, 13 (1985)
16. K. Shimizu, A. Faessler, Nucl. Ph. A**333**, 495 (1980)
17. E. Oset, S.K. Singh, Nucl. Phys. A **542**, 587 (1992)
18. E.K. Warburton, Phys. Rev. C **44**, 233(1991); Phys. Rev. Lett. **66**, 1823 (1991)
19. I.S. Towner, Phys. Lett. B **233**, 13 (1994)
20. W. M. Alberico, M. Ericson, A. Molinari, Nucl. Phys. A**379**, 429 (1982); Ann. Phys. (N.Y.) **154**, 356 (1984)
21. G. Barr, T.K. Gaisser, T. Stanev, Phys. Rev. D**39**, 3532 (1989)
22. T.K. Gaisser, M. Honda, K. Kasahara, H. Lee, S. Midorikawa, V.A. Naumov, T. Stanev, Phys. Rev. D**54**, 5578 (1996)